Results in Physics 8 (2018) 391–396

Contents lists available at ScienceDirect

Results in Physics

journal homepage: www.journals.elsevier.com/results-in-physics

Microstructure and dielectric properties of BZT-BCT/PVDF nanocomposites

Qingguo Chi [a,b,c,*], Guang Liu [a], Changhai Zhang [a], Yang Cui [a,b], Xuan Wang [a,b], Qingquan Lei [a]

[a] Key Laboratory of Engineering Dielectrics and Its Application, Ministry of Education, Harbin University of Science and Technology, Harbin 150080, PR China
[b] School of Electrical and Electronic Engineering, Harbin University of Science and Technology, Harbin 150080, PR China
[c] State Key Laboratory of Electronic Thin Films and Integrated Devices, University of Electronic Science and Technology of China, Chengdu 610054, PR China

ARTICLE INFO

Article history:
Received 3 November 2017
Received in revised form 17 December 2017
Accepted 17 December 2017
Available online 19 December 2017

Keywords:
Powders
Nanocomposites
Interfaces
Dielectric properties
Energy storage density

ABSTRACT

In this paper, the $0.5Ba(Zr_{0.2}Ti_{0.8})O_3$-$0.5(Ba_{0.7}Ca_{0.3})TiO_3$ nanofibers (BZT-BCT NFs) with high aspect ratio were synthesized by electrospinning technique, and the PVDF-based composites filled with the BT NPs or BZT-BCT NFs were fabricated. Obviously, compared to the BT NPs/PVDF composite, the dielectric properties of BZT-BCT NFs/PVDF composites are improved at given volume fraction. The electric modulus formalism indicated that the BZT-BCT NFs could effectively enhance the interfacial polarization of the BZT-BCT NFs/PVDF composites than that of the BT NPs/PVDF composite. In addition, the BZT-BCT NFs with large aspect ratio can make the composites polarize at a higher field strength, thus the composites obtain higher polarization strength. The energy density of 3 vol% BZT-BCT NFs/PVDF composite is 3.08 J/cm^3 at 240 kV/mm, which is 2.01 times higher enhancement than the BT NPs/PVDF composite (1.53 J/cm^3 at 180 kV/mm). These results also provide a simple but effective method to achieve the materials with high capacitance for energy storage.

Introduction

Polymer matrix composites as a kind of flexible functional materials have potential prospects in the field of electronic devices. Owing to the rapid development of the electronics industry, new requirements are presented for the materials [1–8]. Considering the energy storage scope, energy density (U_e) of a material can be calculated by $U = \int EdD$, where E is the electric field and D is the electric displacement ($D = \varepsilon_0\varepsilon_r E$) [9]. According to the above formula, the energy density of material is related to the breakdown strength and dielectric permittivity [10]. The polymer has high breakdown strength and excellent flexibility, but its dielectric properties are not so well ($\varepsilon < 10$) [11,12]. Therefore, the polymer matrix composites with adding inorganic filler is the focus of energy storage applications.

Ceramic materials are widely used in energy storage composites because of their high dielectric permittivity. $BaTiO_3$ (BT), $CaCu_3Ti_4O_{12}$ (CCTO), $Ba_{0.6}Sr_{0.4}TiO_3$ (BST) and other ferroelectric ceramics particles are added to polymer matrix, and the composites possess excellent dielectric properties [13–21]. Yang et al. [14] studied the nano- and micron- sized CCTO doped in poly(vinylidene fluoride) (PVDF) and found that when the content of nano-CCTO filler reached to 40 vol%, the dielectric constant was over 106 at 100 Hz, which was higher than that of the micron-CCTO ($\varepsilon = 35.7$). Moreover, the dielectric loss values of the two samples were 50 and 0.13, respectively. Fu et al. [15] studied the size dependent polarization and surface modification of BT particle and obtained high performance BT/PVDF composites. The results revealed that 600 nm sized BT particles possessed the strong polarization. The composites with 40 vol% BT loading exhibited the largest dielectric constant (65, 25 °C, 1 kHz) and the energy density with 60 vol% was 45.8×10^{-3} J/cm^3 at 10 kV/mm.

Although high dielectric permittivity is obtained by adding ceramic particles, the high content may cause damage to the breakdown strength and lose their flexibility and uniformity [14–18]. Therefore, ceramic particles are not the best choice to improve the energy storage of polymer matrix composites. Recently, more and more reports about that different morphologies and structures of the filling phase are introduced to further improve the properties of the composites. Lou et al. [19] designed the structure and preparation method of the 3D-$BaTiO_3$/epoxy composites, and successfully constructed the three-dimensional high dielectric network in the polymer system. The results show that the dielectric constant of the 3D-$BaTiO_3$/epoxy composites was 200 and the energy storage density is greatly improved when the filler content

* Corresponding author at: Key Laboratory of Engineering Dielectrics and Its Application, Ministry of Education, Harbin University of Science and Technology, Harbin 150080, PR China.
E-mail address: qgchi@hotmail.com (Q. Chi).

https://doi.org/10.1016/j.rinp.2017.12.052
2211-3797/

is only 30 vol%. Tang et al. [20] successfully obtained the BT nanowires and adding them to the P(VDF-TrFE-CFE) matrix. The study found that the BT nanowires with high aspect ratio showed better performance than low aspect ratio. The energy density of the P(VDF-TrFE-CFE) composites reached to 10.48 J/cm^3 at 300 MV/m when the BT nanowires are 17.5 vol%. Similarly, Liu et al. [21] prepared BST60NF/PVDF with a large aspect ratio via electrospinning and employing surface hydroxylated. The nanocomposites exhibited excellent properties and their dielectric constant reached up to 25 at 10 vol% BST60 NF. The maximal energy storage density of nanocomposites with 2.5 vol% BST60 NF was 6.4 J/cm^3 and the efficiency still was higher than 50% at an electric field of 3800 kV/cm. As mentioned in the report, in addition to the design of the composites structure, an important way to improve the properties of the composites is to obtain ceramic nanofibers with large aspect ratio.

Meanwhile, according to previous contributes, there are some modifiers acting as the shell layer to enhanced the interface compatibility and to increase the insulation of inorganic fillers. For instance, Pan et al. used the PATP as the shell layer to increase the insulation of BCZT NF, which could effectively restrict the carrier migration in the composite [2]. Meanwhile, Chi et al. also induced the PDA as modifier to improve the dispersibility of fillers in the PVDF matrix and to alleviate the dielectric difference between fillers and matrix [6]. Yang et al. produced the core–shell structure BT-PDA-Ag by dopamine modification to improve the interface compatibility and to enhance the breakdown strength of dielectric composite [22]. Based on above mentioned literatures, we also used the PDA as surface modification for fillers.

The $0.5Ba(Zr_{0.2}Ti_{0.8})O_3$-$0.5(Ba_{0.7}Ca_{0.3})TiO_3$ ceramic (BZT-BCT) exhibits a very high piezoelectric coefficient of 620 pC/N in its morphotropic phase boundary, and the dielectric constant of BZT-BCT was found to be 3370 at room temperature at 1 kHz frequency [23–26]. In this paper, BZT-BCT nanofibers with large aspect ratio were synthesized by electrospinning technique and uniformly dispersed in the PVDF matrix. The BZT-BCT NFs/PVDF has superior performance compared to BT NPs/PVDF. Therefore, it is believed that the BZT-BCT introduced into the polymer matrix can greatly improve the dielectric properties and energy storage properties of polymer matrix composites.

Materials and methods

The BZT-BCT NFs were prepared via electrospinning technique. All the solvents and raw materials (if there was no special statement, all the materials were supplied by Sinopharm Chemical Reagent Co., China) are analytically pure and without any further purification. Firstly, the 3.80 ml of ethanol, 9.05 ml of acetic acid and 1.54 ml of acetylacetonate were added in a 25 ml erlenmeyer flask and mixed. Then, barium hydroxide ($Ba(OH)_2{\cdot}8H_2O$, 2.172 g), calcium hydroxide ($Ca(OH)_2$, 0.090 g) and zirconium acetylacetonate ($C_{20}H_{28}ZrO_8$, 0.394 g) were sequentially added to the above solution in sequence with vigorous stirring. 2.48 ml of tetrabutyl titanate was added to the mixed solution under vigorous stirring for 30 min to form stable and uniform electrospinning precursor sol. Subsequently, polyvinylpyrrolidone (PVP, M_w = 1,300,000, Aladdin) was used to adjust the viscosity of the sol to a proper value before transferring the sol into a syringe. Then, the precursor was electrospun into nanofibers under a high voltage of 30 kV with a propulsion rate of 0.1 ml/min. The distance between the needle tip and the collector was about 25 cm, and the temperature and humidity were about 20 °C and 30%, respectively. Finally, BZT-BCT NFs were obtained by calcinated the as-electrospun fiber in a muffle furnace at 700 °C for 3 h.

Before preparing the composites, the 1 g BZT-BCT NFs were dispersed in the Tris-HCl aqueous solution (2 mg/mL, pH = 8.5, Aladdin) followed by sonication for 30 min; then 0.2 g PDA (Aladdin) was added and stirred vigorously at room temperature for 12 h. The nanofibers were then extracted from the solution with centrifugation and washed alternately with deionized water and ethanol for three times. Finally, the nanofibers were dried at 80 °C for 12 h. For the preparation of nanocomposite films, the BZT-BCT NFs and PVDF (Shanghai 3F New Material Co., Ltd., China) were dissolved into N, N-dimethylformamide (DMF) and stirred for 24 h at room temperature for the homogeneous mixing. Upon completion, the mixture was casted onto a clean glass plate and the films were dried at 60 °C for 12 h. Finally, the BZT-BCT NFs/PVDF composite films were obtained with the thickness of about 25 μm. For comparison, we choose the barium titanate (BT) nanoparticles (200 nm, Shandong Sinocera Functional Material Co., Ltd., China.) as the filler to prepare the BT NPs/PVDF composite films in the same procedure.

X-ray diffraction (XRD, Empyrean) was carried out to investigate the crystal structure of the samples using Cu Kα radiation (λ = 1.5418 Å) at 40 kV and 40 mA. The microstructure of the BT nanoparticles, BZT-BCT nanofibers and PVDF-based composite films were determined using scanning electron microscopy (SEM, Hitachi S-3400N). The dielectric properties of the PVDF-based composites were determined in the frequency range of 0.1 Hz to 1 MHz at room temperature using a broadband dielectric spectral instrument (Novocontrol Alpha-A). Prior to performing dielectric measurements, a layer of Al paste (diameter 25 mm) was evaporated on both surfaces to serve as electrodes. Energy storage density of the composites was measured by a Precision Premier ferroelectric polarization tester (Radiant, Inc.) at room temperature and 10 Hz using the same samples prepared for dielectric properties testing.

Results and discussion

XRD patterns of BT NPs and BZT-BCT NFs are given in Fig. 1a and b, respectively. Compared to the pure BT NPs, it was shown that the characteristic diffraction peaks of BZT-BCT appear at 2θ = 22°, 31°, 39°, 45°, and 56°, corresponding to (1 0 0), (1 1 0), (1 1 1), (2 0 0), and (2 1 1), respectively. The characteristic diffraction peaks were assigned to BZT-BCT with a pseudo-cubic structure. No visible signal of the presence of secondary phases was observed. The morphologies of the BT NPs and BZT-BCT NFs were directly illustrated by SEM images, as shown in the inset of Fig. 1(a1 and b1). The BT NPs consisted of spherical particles with the grain size of about 200 nm. By contrast, the SEM image revealed that the BZT-BCT NFs had the large aspect ratio and favorable dispersibility, for instance, diameters of 250 nm–300 nm and lengths of 2 μm–3.5 μm.

Next, the PVDF-based composite films filled with the BT NPs and BZT-BCT NFs were prepared, and the XRD patterns of BT NPs/PVDF and BZT-BCT NFs/PVDF composite films were presented in Fig. 2. For the all composites, the XRD pattern of pure PVDF appeared at about 2θ = 17.76°, 19.81° [27], When the fillers were incorporated into PVDF matrix, the peaks of PVDF showed an evident reduction in intensity. With the fraction of fillers increasing, the peaks of PVDF reduced gradually, while those of BT NPs and BZT-BCT NFs became sharper and stronger. The main reason was that, by adding the ceramic filler, the orderly arrangement of the molecular structure of the PVDF was destroyed, reducing the arrangement density of molecular chain. The XRD patterns of the composites showed BT, BZT-BCT, and PVDF diffraction peaks, which clearly demonstrated that the BT NPs and BZT-BCT NFs filled in the polymer matrix and without other impurities.

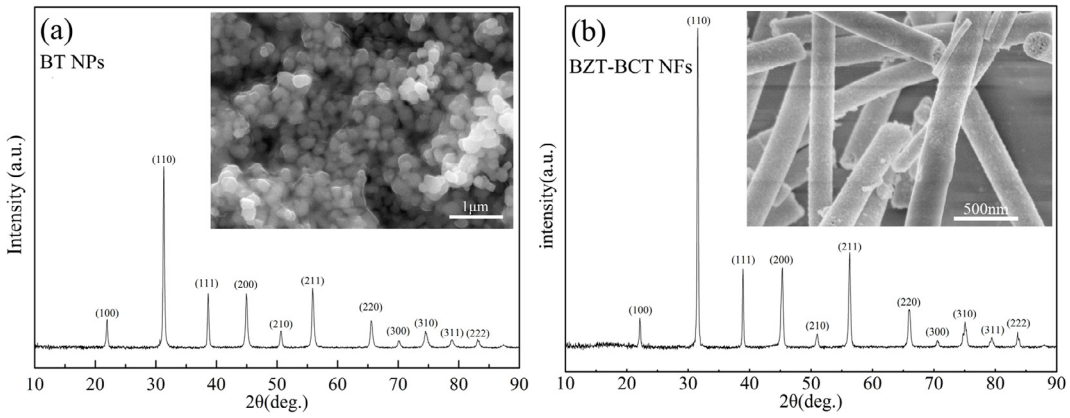

Fig. 1. XRD patterns of the (a) BT NPs and (b) BZT-BCT NFs. The inset of the (a) and (b) show the SEM image of the BT NPs and BZT-BCT NFs, respectively.

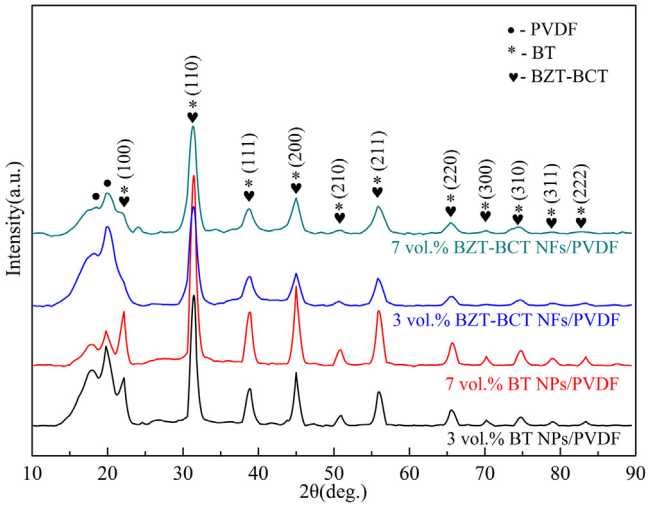

Fig. 2. XRD patterns of BT NPs/PVDF and PVDF/BZT-BCT NFs composites.

The cross-sectional SEM images of 3 vol% BT NPs/PVDF, 7 vol% BT NPs/PVDF, 3 vol% BZT-BCT NFs/PVDF and 7 vol% BZT-BCT NFs/PVDF composite films are shown in Fig. 3a–d, respectively. It can be observed that all the BT NPs and BZT-BCT NFs exhibit good compatibility and dispersibility in the PVDF matrix without obvious agglomeration. This can be attributed to that the fact that the fillers were surface modified by dopamine and therefore forming a strong adhesive bonding force with the polymer matrix. In addition, as shown in Fig. 3d, the BZT-BCT NFs are randomly homogeneously dispersed and tend to be oriented in the in-plane direction in the nanocomposites and remain in high aspect ratio [28].

For comparison, the dependence of the dielectric constant, dielectric loss tangent and conductivity of nanocomposite films with different contents of the BT NPs and BZT-BCT NFs were measured, as displayed in Fig. 4. It is noteworthy that the dielectric constant of the composite films increases monotonously with increasing of the filler content, especially in frequency range of 0.1–100 Hz. Besides, the dielectric constant of the BT NPs/PVDF composite films is inferior to those of BZT-BCT NFs/PVDF composite films at the same filler loading, which clearly demonstrated that the addition of BZT-BCT NFs can significantly improve the dielectric constant of the composites. In particular, the dielectric constant of the 7 vol% BZT-BCT NFs/PVDF composite films is about 78.46 at 0.1 Hz, which is 2.3 times higher than that (34.06) of composites filled by BT NPs. This feature possibly results from the stronger interfacial polarization existing in the BZT-BCT NFs/PVDF composite films, and the interfacial polarization on the dielectric constant decreases with the increasing frequency [29–31].

The dielectric loss tangent measured at a given frequency including polarization loss and conduction loss. Fig. 4b displayed the dependence of dielectric loss tangent as function of frequency for BT NPs/PVDF and BZT-BZT NFs/PVDF composites with different filler contents. It can be found that the loss tangent of the composite films decreased at the low frequency and then increased with the further increasing of frequency. It showed the relaxation properties of the dielectric materials, including the Maxwell-Wagner (M–W) relaxation and α relaxation of PVDF at low and high frequencies, respectively [32–34]. Besides, for the BZT-BZT NFs/PVDF composites, the decreasing trend of the dielectric loss tangent was larger than that of BT NPs/PVDF composites at low frequency. It is generally believed that the interfacial polarization and conductivity are contributed significantly to the dielectric response at low frequency, and the interfacial polarization in the BZT-BZT NFs/PVDF composites should be much stronger than those in BT NPs/PVDF composites.

To make a thorough inquiry about the insulation properties of composite materials, the conductivities of the BT NPs/PVDF and BZT-BZT NFs/PVDF composites are given in Fig. 4c. It can be found that the conductivity of the all composites is strongly dependent on the frequency, which indicates that the composite films show good insulation properties. In addition, the conductivity of the composites increases with the increase of the filler content in the whole frequency range. The conductivity of 7 vol% BZT-BCT NFs/PVDF composite is 4.6053×10^{-12} S/cm at 0.1 Hz, which is much greater than that of 7 vol% BT NPs/PVDF composites (1.7508×10^{-12} S/cm). This may be due to the shaper and the high aspect ratio of BZT-BCT NFs, which make the NFs easier to reach the percolation threshold value than that of NPs in the PVDF matrix [18].

More detailed information can be obtained about the influence of the BT NPs and the BZT-BCT NFs on the interfacial polarization between the polymer matrix and fillers. To clarify the mechanism of the dielectric behaviors of the BT NPs/PVDF and BZT-BCT NFs/PVDF composites, an electric modulus formalism based analysis of the dielectric relaxation in the composites has been proposed. Complex dielectric modulus formalism M^* is demonstrated as follows [35–37]:

$$M^* = \frac{1}{\varepsilon^*} = \frac{1}{\varepsilon' - j\varepsilon''} = \frac{\varepsilon'}{\varepsilon'^2 + \varepsilon''^2} + j\frac{\varepsilon''}{\varepsilon'^2 + \varepsilon''^2} = M' + jM'' \quad (1)$$

where M'' is the imaginary part of the electric modulus. The imaginary part M'' of the electric modulus takes the form of loss curves, allowing us to interpret the relaxation phenomena. Because the relaxation time of interfacial polarization is considerably long, the

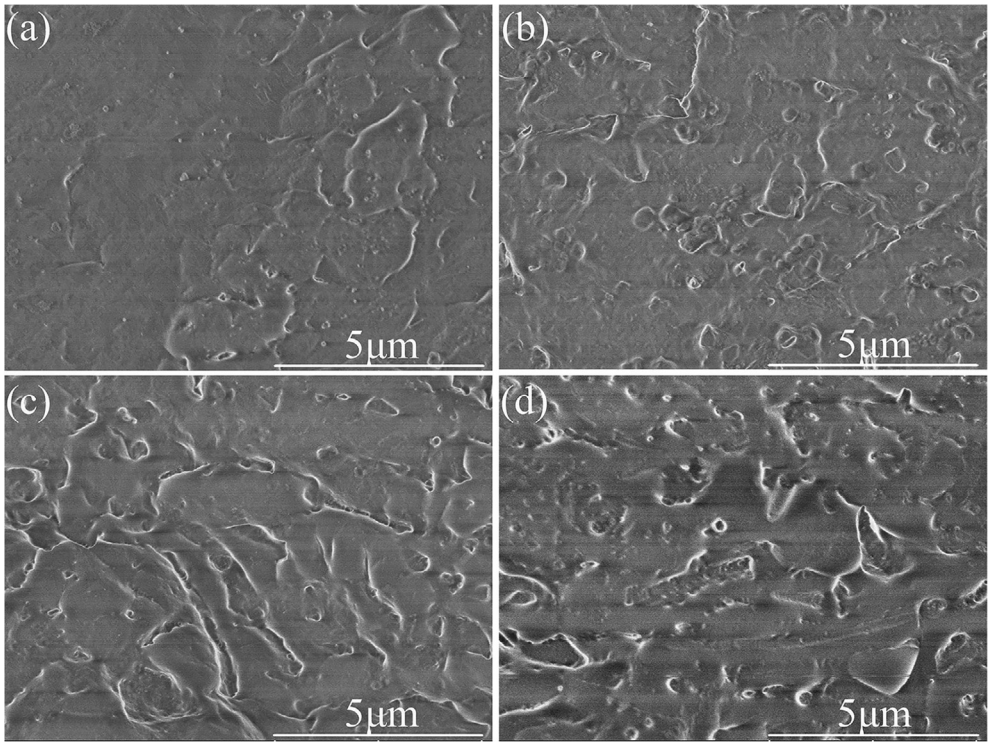

Fig. 3. Cross-sectional SEM images of (a) 3 vol% BT NPs/PVDF (b) 7 vol% BT NPs/PVDF (c) 3 vol% BZT-BCT NFs/PVDF (d) 7 vol% BZT-BCT NFs/PVDF composite films.

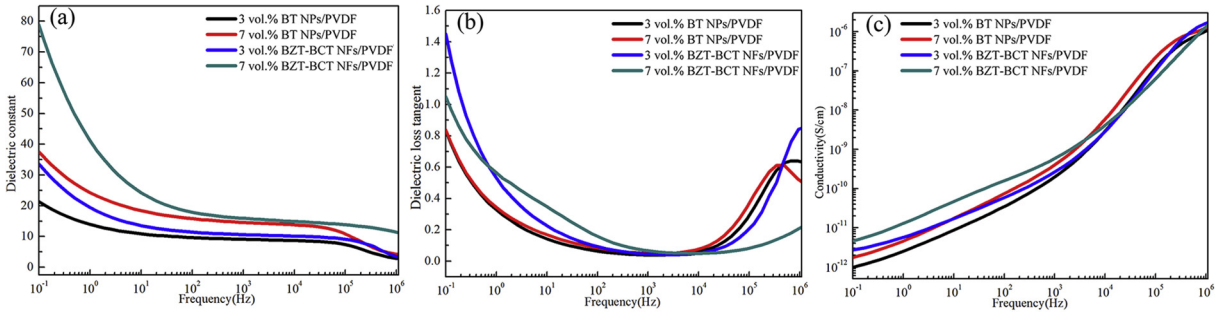

Fig. 4. Dependence of the (a) dielectric constant, (b) dielectric loss tangent, (c) conductivity of BT NPs/PVDF and BZT-BCT NFs/PVDF composites with different filler contents on the frequency at room temperature.

peak of M'' at lower frequency represents the interfacial polarization. Fig. 5 displays the frequency-dependence M'' of the BT NPs/PVDF and BZT-BCT NFs/PVDF composites with different filler contents. For the BT NPs/PVDF composites, we can see that the relaxation strength decreases with the increase of the BT NPs, whereas the relaxation peak frequency and relaxation range almost do not have change, indicating that the interfacial polarization only appears at low frequencies in BT NPs/PVDF composites. For the BZT-BCT NFs/PVDF composites, it can be obviously observed that the interfacial polarization relaxation peaks become broader and shift to high frequency with the increase of filler loading, indicating that the incorporation of BZT-BCT NFs increases the interfacial polarization in the composites. It should be noted that a few voids would be formed when the decomposition and carbonization of organic precursors in the as-spun nanofibers during the heat treatment, and these voids will be remained during the grains growth of the BZT-BCT NFs. These voids can generate charge carriers, which significantly improve the space charge accumulation in the polymer matrix [37–39].

One of the important applications of the high dielectric constant composites is the energy storage devices. The energy storage densities of the BT NPs/PVDF and BZT-BCT NFs/PVDF composite films with different filler contents are shown in Fig. 6. Clearly, the energy density increases with the increasing content of fillers under the same electric field. This is mainly ascribed to the large dielectric constant of the fillers that has large electric displacement. Compared to BT NPs/PVDF composites, a higher energy density of the BZT-BCT NFs/PVDF composites can be achieved at the same condition. The composites with NFs may have a higher breakdown electric field compared to the composites with NPs, which could be explained by the following three reasons. The first is that the NFs can be uniformly dispersed in the PVDF matrix to reduce the percolative pathways for the charge transfer and to suppress the mobility of the polymer chains. The second one is the NFs in the matrix could restrain the growth of electrical treeing by bringing up twisted pathways for treeing, which act as scattering centers for the charge carriers within the composites. The high electric field composites may be polarized at the higher field, which illustrates that the composites can obtain higher polarization at high

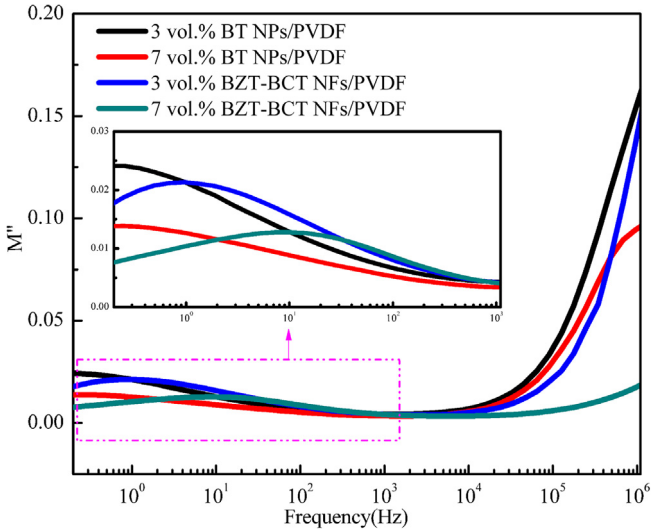

Fig. 5. Frequency-dependence of the imaginary part of the electric modulus for BT NPs/PVDF and BZT-BCT NFs/PVDF composites with different filler contents on the frequency at room temperature.

field. Based on this, the energy storage density of the nanocomposite with the 3 vol% BZT-BCT NFs is up to 3.08 J/cm^3 at an electric field of 240 kV/mm, about 201% higher than that with BT NPs at an electric field of 180 kV/mm (Fig. 6(a)). Noted that the energy storage density of composites is also enhanced with the increasing content of filler. However, due to the high content of the filler in the composites, there are some defects and voids in the composite films. And the high dielectric constant fillers distort the distribution of the electric filed, resulting in the significant decrease of the breakdown strength of the composites [30].

In practical application, apart from higher energy storage density values, larger energy-storage efficiency is also desired. As plotted in Fig. 6, the η of composite decreases with the increasing filler contents at the same electric field, which may be due to the enhanced ferroelectric loss and conduction loss. Compared to the BT NPs/PVDF composites, the BZT-BCT NFs/PVDF composites have a better efficiency at the same electric field. At an electric field of 180 kV/mm, the energy efficiency for the nanocomposites with 3 vol% BZT-BCT NFs and BT NPs is 69% and 67.1%, respectively. It is clearly indicated that the nanocomposites with the BZT-BCT NFs exhibit much higher discharged energy-storage density and show much higher energy efficiency in comparison with nanocomposite with the BT NPs.

Conclusion

In summary, the BZT-BCT NFs were synthesized by electrospinning technique, and the PVDF-based composites filled by the BT NPs or BZT-BCT NFs were fabricated. The XRD and SEM images provided the evidence that the BZT-BCT NFs had a pseudo-cubic structure and a high aspect ratio. The dielectric constant of the BZT-BCT NFs/PVDF composite was obviously larger than that of BT NPs/PVDF composite. The electric modulus formalism indicated that the BZT-BCT NFs could effectively enhance the interfacial polarization of the BZT-BCT NFs/PVDF composites than that of BT NPs/PVDF composite. In addition, the BZT-BCT NFs with large aspect ratio could make the composites polarize at a higher field strength, thus the composites obtained a higher polarization strength. The energy density of 3 vol% BZT-BCT NFs/PVDF composites is 3.08 J/cm^3 at 240 kV/mm, and the efficiency is also kept at 60.56%. These results also provide a simple but effective method to achieve the materials with high capacitance for energy storage.

Acknowledgments

The authors gratefully acknowledge the support of the National Natural Science Foundation of China (61640019), the Open Foundation of State Key Laboratory of Electronic Thin Films and Integrated Devices (KFJJ201601), the Youth Innovative Talents Training Plan of Ordinary Undergraduate Colleges in Heilongjiang (UNPYSCT-2016157), Science Funds for the Young Innovative Talents of HUST (201102).

References

[1] Li Q, Chen L, Gadinski MR, Zhang S, Zhang G, Li H, Haque A, Chen LQ, Jackson T, Wang Q. Flexible high-temperature dielectric materials from polymer nanocomposites. Nature 2015;523:576–9.
[2] Pan Z, Yao L, Zhai J, Wang H, Shen B. Ultrafast discharge and enhanced energy density of polymer nanocomposites loaded with 0.5($Ba_{0.7}Ca_{0.3}$)TiO_3-0.5Ba($Zr_{0.2}Ti_{0.8}$)O_3 one-dimensional nanofibers. ACS Appl Mater Interfaces 2017;9:14337–46.
[3] Dang ZM, Yuan JK, Yao SH, Liao RJ. Flexible nanodielectric materials with high permittivity for power energy storage. Adv Mater 2013;25:6334–665.
[4] Bhavanasi V, Kumar V, Parida K, Wang J, Lee PS. Enhanced piezoelectric energy harvesting performance of flexible PVDF-TrFE bilayer films with graphene oxide. ACS Appl Mater Interfaces 2016;8:521–9.
[5] Prateek VK, Thakur RK. Gupta, Recent progress on ferroelectric polymer-based nanocomposites for high energy density capacitors: synthesis, dielectric properties, and future aspects. Chem Rev 2016;116:4260–317.
[6] Chi Q, Ma T, Zhang Y, Cui Y, Zhang C, Lin J, Wang X, Lei Q. Significantly enhanced energy storage density for poly(vinylidene fluoride) composites by induced PDA-coated 0.5Ba($Zr_{0.2}Ti_{0.8}$)O_3-0.5($Ba_{0.7}Ca_{0.3}$)TiO_3 nanofibers. J Mater Chem A 2017;5:16757–66.

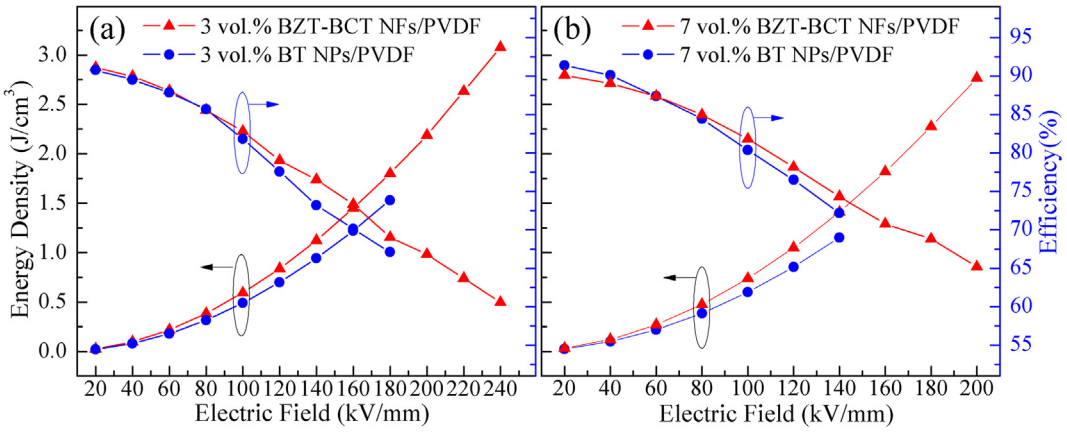

Fig. 6. Energy density and efficiency of the BT NPs/PVDF and PVDF/BZT-BCT NFs composites. (a) 3 vol%, and (b) 7 vol%.

[7] Arun MK, Treich GM, Huan TD, Ma R, Tefferi M, Cao Y, Sotzing GA, Ramprasad R. Rational Co-design of polymer dielectrics for energy storage. Adv Mater 2016;28:6277–91.
[8] Zhang Y, Chi Q, Liu L, Zhang C, Chen C, Wang X, Lei Q. Enhanced electric polarization and breakdown strength in the all-organic sandwich-structured poly(vinylidene fluoride)-based dielectric film for high energy density capacitor. APL Mater 2017;5:076109.
[9] Fan YY, Huang XY, Wang GY, Jiang PK. Core-shell structured biopolymer@$BaTiO_3$ nanoparticles for biopolymer nano-composites with significantly enhanced dielectric properties and energy storage capability. J Phys Chem C 2015;119:27330–9.
[10] Khanchaitit P, Han K, Gadinski MR, Li Q, Wang Q. Ferroelectric polymer networks with high energy density and improved discharged efficiency for dielectric energy storage. Nat Commun 2013;4:2845.
[11] Wu S, Lin MR, Lu SG, Zhu L, Zhang QM. Polar-fluoropolymer blends with tailored nanostructures for high energy density low loss capacitor applications. Appl Phys Lett 2011;99:132901.
[12] Yu K, Wang H, Zhou YC, Bai YY, Niu YJ. Enhanced dielectric properties of $BaTiO_3$/poly(vinylidene fluoride) nano-composites for energy storage applications. J Appl Phys 2013;113:034105.
[13] Chi QG, Dong JF, Zhang CH, Wang X, Lei QQ. Highly (100)-oriented sandwich structure of $(Na_{0.85}K_{0.15})_{0.5}Bi_{0.5}TiO_3$ composite films with outstanding pyroelectric properties. J Mater Chem C 2016;4:4442–50.
[14] Yang WH, Yu SH, Sun R, Du RX. Nano- and microsize effect of CCTO fillers on the dielectric behavior of CCTO/PVDF composites. Acta Mater 2011;59:5593–602.
[15] Fu J, Hou YD, Zheng MP, Wei QY, Zhu MK, Yan H. Improving dielectric properties of PVDF composites by employing surface modified strong polarized $BaTiO_3$ particles derived by molten salt method. ACS Appl Mater Interfaces 2015;7:24480–91.
[16] Huang XY, Jiang P. Core-shell structured high-*k* polymer nanocomposites for energy storage and dielectric applications. Adv Mater 2015;27:546–54.
[17] Luo SB, Yu SH, Sun R, Wong CP. Nano Ag-deposited $BaTiO_3$ hybrid particles as fillers for polymeric dielectric composites: toward high dielectric constant and suppressed loss. ACS Appl Mater Interfaces 2014;6:176–82.
[18] Chi QG, Dong JF, Zhang CH, Wong CP, Wang X, Lei QQ. Nano iron oxide-deposited calcium copper titanate/polyimide hybrid films induced by an external magnetic field: toward a high dielectric constant and suppressed loss. J Mater Chem C 2016;4:8179–88.
[19] Luo SB, Shen YB, Yu SH, Wan YJ, Liao WH, Sun RS, Wong CP. Construction of a 3D-$BaTiO_3$ network leading to significantly enhanced dielectric permittivity and energy storage density of polymer composites. Energy Environ Sci 2017;10:137–44.
[20] Tang HX, Lin YR, Sodano HA. Synthesis of high aspect ratio $BaTiO_3$ nanowires for high energy density nanocomposite capacitors. Adv Energy Mater 2013;3:451–6.
[21] Liu SH, Zhai JW, Wang JW, Xue SX, Zhang WQ. Enhanced energy storage density in poly(vinylidene fluoride) nanocomposites by a small loading of suface-hydroxylated $Ba_{0.6}Sr_{0.4}TiO_3$ nanofibers. ACS Appl Mater Interfaces 2016;6:1533–40.
[22] Yang K, Xingyi H, Jinliang H, Pingkai J. Strawberry-like core-shell Ag@polydopamine@$BaTiO_3$ hybrid nanoparticles for high-k polymer nanocomposites with high energy density and low dielectric loss. Adv Mater Interfaces 2016;2(17):1500361–71.
[23] Liu W, Ren X. Large piezoelectric effect in Pb-free ceramics. Phys Rev Lett 2009;103:257602.
[24] Mishra P, Sonia Kumar P. Effect of sintering temperature on dielectric, piezoelectric and ferroelectric properties of BZT–BCT 50/50 ceramics. J Alloy Compd 2012;545:210–5.
[25] Zhang CH, Chi QG, He XX, Lin JQ, Chen Y, Liu LZ, Lei QQ. Microstructure and electric properties of Nb doping $x(Ba_{0.7}Ca_{0.3})TiO_3$-$(1-x)Ba(Zr_{0.2}Ti_{0.8})O_3$, ceramics. J Alloy Compd 2016;685:936–40.
[26] Chi QG, Dong JF, Liu GY, Chen Y, Wang X, Lei QQ. Effect of particle size on the dielectric properties of $0.5Ba(Zr_{0.2}Ti_{0.8})O_3$–$0.5(Ba_{0.7}Ca_{0.8})TiO_3$/polyvinylidene fluoride hybrid films. Ceram Int 2015;41:15116–21.
[27] Ma WZ, Zhang J, Chen SQ, Wang XL. β-Phase of poly(vinylidene fluoride) formation in poly(vinylidene fluoride)/poly(methyl methacrylate) blend from solutions. Appl Surf Sci 2008;254:5635–42.
[28] Lee H, Dellatore SM, Miller WM, Messersmith PB. Mussel-inspired surface chemistry for multifunctional coatings. Science 2007;318:426–30.
[29] Chen Q, Shen Y, Zhang SH, Zhang QM. Polymer-based dielectrics with high energy storage density. Annu Rev Mater Res 2015;45:433–58.
[30] Pan ZB, Yao LM, Zhai JW, Fu DZ, Shen B, Wang HT. High energy density polymer nanocomposites composed of newly structured one-dimensional $BaTiO_3$@Al_2O_3 nanofibers. ACS Appl Mater Interfaces 2017;9:4024.
[31] Zha JW, Meng X, Wang DG, Dang ZM. Robert K.Y. Li. Dielectric properties of poly(vinylidene fluoride) nanocomposites filled with surface coated $BaTiO_3$ by SnO_2 nanodots. Appl Phys Lett 2014;104:072906.
[32] Zhang CH, Chi QG, Dong JF, Cui Y, Wang X, Lei QQ. Enhanced dielectric properties of poly(vinylidene fluoride) composites filled with nano iron oxide-deposited barium titanate hybrid particles. Sci Rep 2016;6:33508.
[33] Fang F, Yang WH, Yu SH, Luo SB, Sun R. Mechanism of high dielectric performance of polymer composites induced by $BaTiO_3$-supporting Ag hybrid fillers. Appl Phys Lett 2014;104:576.
[34] Chen ST, Yao K, Tay FEH, Liow CL. Ferroelectric poly(vinylidene fluoride) thin films on Si substrate with the β phase promoted by hydrated magnesium nitrate. J Appl Phys 2007;102. 104108-104108-7.
[35] Wu W, Huang XY, Li ST, Jiang PK, Toshikatsu T. Novel three-dimensional zinc oxide superstructures for high dielectric constant polymer composites capable of withstanding high electric field. J Phys Chem C 2012;116:24887–95.
[36] Liu SH, Wang J, Shen B, Zhai JW. Poly(vinylidene fluoride) nanocomposites with a small loading of core-shell structured $BaTiO_3$@Al_2O_3, nanofibers exhibiting high discharged energy density and efficiency. J Alloy Compd 2016;696:585–9.
[37] Li Y, Huang XY, Hu ZW, Jiang PK, Li ST, Tanaka T. Large dielectric constant and high thermal conductivity in poly(vinylidene fluoride)/barium titanate/silicon carbide three-phase nanocomposites. ACS Appl Mater Interfaces 2016;3:4396–403.
[38] Pan ZB, Yao LM, Zhai JW, Shen B, Liu SH, Wang HT, Liu JH. Excellent energy density of polymer nanocomposites containing $BaTiO_3$@Al_2O_3 nanofibers induced by moderate interfacial area. J Mater Chem A 2016;4:13259–64.
[39] Dang ZM, Zheng MS, Zha JW. 1D/2D carbon nanomaterial-polymer dielectric composites with high permittivity for power energy storage applications. Small 2016;12:1688–701.